SANDIA REPORT
SAND2019-14935
Printed December 2019

Sandia National Laboratories

Asymmetric Double Cantilever Beam Test to Measure the Toughness of an Alumina/Epoxy Interface

M. E. Stavig, R. Jaramillo, E.C. Larkin, J.W. Dugger, and E.D. Reedy

Prepared by
Sandia National Laboratories
Albuquerque, New Mexico
87185 and Livermore,
California 94550

Issued by Sandia National Laboratories, operated for the United States Department of Energy by National Technology & Engineering Solutions of Sandia, LLC.

Available to DOE and DOE contractors from
U.S. Department of Energy
Office of Scientific and Technical Information
P.O. Box 62
Oak Ridge, TN 37831

Telephone: (865) 576-8401
Facsimile: (865) 576-5728
E-Mail: reports@osti.gov
Online ordering: http://www.osti.gov/scitech

Available to the public from
U.S. Department of Commerce
National Technical Information Service
5301 Shawnee Rd
Alexandria, VA 22312

Telephone: (800) 553-6847
Facsimile: (703) 605-6900
E-Mail: orders@ntis.gov
Online order: https://classic.ntis.gov/help/order-methods/

ABSTRACT

This report describes an adhesively bonded, Asymmetric Double Cantilever Beam (ADCB) fracture specimen that has been expressly developed to measure the toughness of an alumina (Al_2O_3)/epoxy interface. The measured interfacial fracture toughness quantifies resistance to crack growth along an interface with the stipulation that crack-tip yielding is limited and localized to the crack-tip. An ADCB specimen is a variant of the well-known double cantilever beam specimen, but in the ADCB specimen the two beams have different bending stiffnesses.

This report begins with a brief overview of how crack-tip mode mixity (i.e., a measure of shear-to-normal stress at the crack-tip) is a distinguishing feature of interfacial fracture. Which is then followed by a detailed description of relevant design, fabrication, testing, and associated data analysis techniques. The report then concludes by presenting illustrative results that compare the measured interfacial toughness of an alumina/epoxy interface when the alumina is silane-coated and when the alumina is not silane coated.

This page left blank

CONTENTS

1. Introduction 9
2. Adhesively Bonded Asymmetric Double Cantilever Beam Specimen 11
   2.1. Adhesively Bonded Asymmetric Double Cantilever Beam Specimen Designed to Measure the Toughness of an Al_2O_3/Epoxy Interface 11
3. Fabrication 15
   3.1. Adhesively Bonded Asymmetric Double Cantilever Beam Materials 15
   3.2. Process Al_2O_3 Beam 16
   3.3. Process Kovar Beam 17
   3.4. Adhesively Bond Beams to Form ADCB Specimen 18
4. Test Procedures 19
   4.1. Pre-crack Asymmetric Double Cantilever Beam and Bond on Clevis Adaptor Block 19
   4.2. Test Set Up 20
   4.3. Data Acquisition 20
5. Data Reduction 21
   5.1. Theory 21
   5.2. Procedure 24
6. Example Asymmetric Double Cantilever Beam-Measured Al_2O_3/Epoxy Toughness Data 27
7. Conclusion 30

Appendix A. Spreadsheet To Aid in the Design of ADCB Specimens 32

Appendix B. Spreadsheet that Calculates Toughness 34

LIST OF FIGURES

Figure 1. Plot of Swadener and Liechti Data [8] for an Epoxy/Glass Interface. 10
Figure 2. Schematic of an Adhesively Bonded Asymmetric Double Cantilever Beam. 11
Figure 3. Adhesively Bonded Asymmetric Double Cantilever Beam Specimen with a 0.1 Inch Thick Al_2O_3 Upper Beam and a 0.185 Inch Thick Kovar Lower Beam. 15
Figure 4. Drawing Defining Al_20_3 Upper Beam (Inches) 15
Figure 5. Drawing Defining Kovar Lower Beam (Inches). 16
Figure 6. Pencil Blast Sweep Pattern: -45°, 45°, and Circular. 17
Figure 7. Asymmetric Double Cantilever Beam Specimen Pinned to Load Train. 19
Figure 8. ADCB Sample Mounted in LVDT Holder. 20
Figure 9. Example of the Measured Load vs. Load-Point Displacement Data. 22
Figure 10. Definition of Loading Slope and Critical Load. 23
Figure 11. Example of a Questionable Load vs. Load-Point Displacement Data. 25
Figure 12. Measured Interfacial Toughness of an Al_20_3 Epoxy Interface: Average. 27
Figure 13. Measured Interfacial Toughness of an Al_20_3/Epoxy Interface: All Data Points. 28

LIST OF TABLES

Table 1. Critical Load and Loading Slope Data. 24

LIST OF EQUATIONS

Equation 1 21
Equation 2 23
Equation 3 30

ACRONYMS AND DEFINITIONS

Abbreviation	Definition
Al_20_3	alumina
ADCB	Asymmetric Double Cantilever Beam
C	Celsius
CTE	coefficient of thermal expansion
DAQ	data acquisition
DCB	double cantilever beam
lbf	Foot pound-force
LEFM	Linear Elastic Fracture Mechanics
LVDT	Linear Variable Differential Transformer
psi	pounds per square inch
SNL	Sandia National Laboratories
UHP	ultrahighpure

This page left blank

1. INTRODUCTION

Electrical and mechanical components often contain polymer-solid interfaces and such interfaces can have a significant impact on the component's performance and reliability. For example, a crack (i.e., delamination) between an encapsulant and a high voltage element can lead to dielectric breakdown and component failure. Since small, pre-existing interfacial flaws are often assumed to be unavoidable (and difficult to quantify), it is desirable to fabricate components with interfaces that tend to resist the growth of such flaws. Interfacial fracture toughness Γ quantifies resistance to crack growth along an interface with the stipulation that crack-tip yielding is sufficiently small (i.e., when Linear Elastic Fracture Mechanics (LEFM) is applicable [1, 2]). In LEFM, energy release rate G measures the energy available for an increment of crack extension and a pre-existing crack begins to propagate when G equals the interfacial toughness Γ (sometimes this critical value of G is referred to as G_c). One can think of G as the crack driving force. It is a calculated quantity that depends on applied load, geometry, and elastic properties. Interfacial toughness Γ is a measured quantity that quantifies the resistance to crack growth. The crack growth criterion is $G \geq \Gamma$. Interfacial toughness can be used as a measure of bond quality as well as a primary input in finite element simulations of crack growth in adhesively bonded and encapsulated structures. Interfacial toughness depends on many variables including: test temperature, rate of loading, interfacial surface roughness, and interfacial chemistry. One way of tailoring interfacial chemistry is to apply a silane coating. Such coupling agents introduce covalent bonds in an interphase that can increase interfacial strength and durability [3]. Interfacial toughness also depends on the level of crack-tip energy dissipation (e.g., yielding) that occurs in the adjacent bulk materials. The relationship between toughness values and the parameters that control toughness is in general unknown and must be determined through extensive testing. There has been some recent limited success in reducing this testing burden using a model that relates interfacial toughness, interfacial roughness, and test temperature for some types of aluminum/epoxy interfaces [4].

There are numerous methods for measuring interfacial toughness [5, 6]. One aspect of interfacial fracture mechanics that distinguishes it from traditional LEFM is the role of crack-tip mode-mixity [5]. In a homogeneous, isotropic material, a crack will propagate along a path with a purely tensile, Mode I opening at the crack tip (i.e., there is no Mode II crack-tip shear directly ahead of the crack) [7]. For this reason, only the Mode I toughness is typically relevant in bulk fracture. On the other hand, when there is a material interface and there is relatively weak interfacial bonding, a crack may be constrained to propagate along the interface. In such cases, elastic asymmetry generates both

normal and shear stress on the interface even when the loading is symmetric, and the crack propagates under a mix of Mode I and Mode II. In a further complication, the ratio of interfacial shear to tensile stress changes with distance from the crack tip [5]. Any accurate theory of interfacial cracking must include crack growth under a combined Mode I/Mode II loading.

The level of crack-tip mode-mixity $\psi_{r=l}$ (defined as the arctangent of the ratio of the shear stress to normal stress at a fixed distance l in front of the crack tip in the region dominated by the stress singularity) depends on the mismatch in elastic properties as well as specimen geometry and loading. Mode-mixity is important because the value of the interfacial toughness depends on the level of mode-mixity. Figure 1 plots results published by Swadener and Liechti [8] for an epoxy/glass interface that illustrate how measured interfacial toughness Γ can increase substantially with mode-mixity (measured toughness data plotted as symbols).

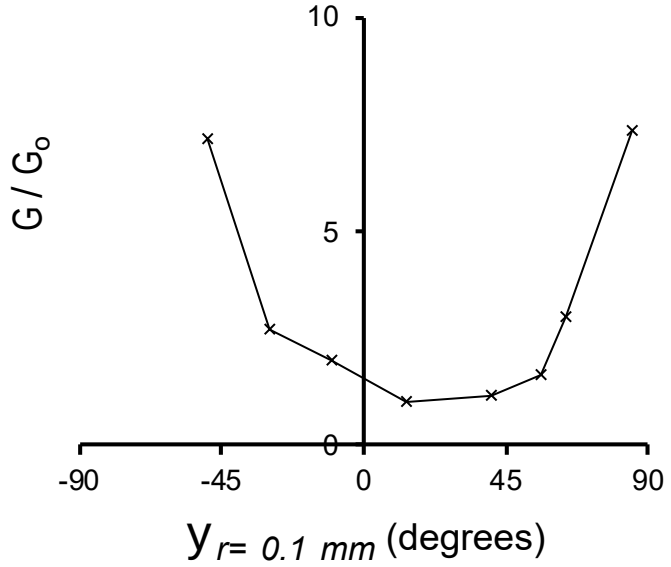

Figure 1. Plot of Swadener and Liechti Data [8] for an Epoxy/Glass Interface.
Note: This figure illustrates how measured interfacial toughness Γ (normalized by the minimum measured toughness Γ_o) varies with crack-tip mode-mixity $\psi_{r=0.1\ mm.}$

Consequently, when one reports an interfacial toughness value, one should also report the mode-mixity of the test specimen used to make the measurement (e.g., Γ at $\psi_{r=l}$, where l is the characteristic length where the mode mixity is defined).

2. ADHESIVELY BONDED ASYMMETRIC DOUBLE CANTILEVER BEAM SPECIMEN

This section describes an adhesively bonded ADCB specimen that has been specifically developed to measure the toughness of Al_2O_3/epoxy interfaces. Detailed descriptions of the relevant design, fabrication, testing, and associated data analysis techniques are presented below. An ADCB specimen (see Figure 2) is a variant of the well-known double cantilever beam (DCB) specimen [1, 2], but in the ADCB specimen the two beams have different bending stiffnesses [9].

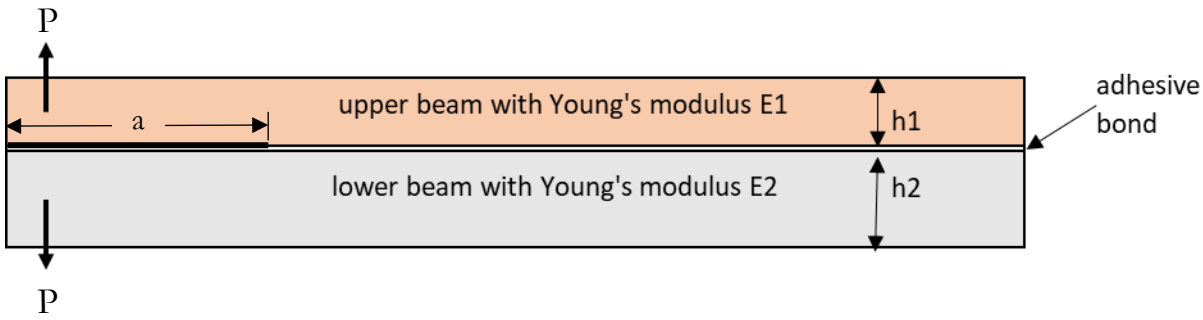

Figure 2. Schematic of an Adhesively Bonded Asymmetric Double Cantilever Beam.

For specificity in the following discussion, the interface crack is assumed to lie between the upper beam and the adhesive bond, and the bending stiffness of the upper beam is assumed to be less than that of the lower beam ($E_1h_1^3 < E_2h_2^3$). One virtue of the ADCB specimen is that multiple toughness measurements can be made using a single sample since for a fixed load point displacement, the energy release rate G (i.e., crack driving force) decreases as crack length a increases. The ADCB specimen is loaded by pulling the ends apart to propagate a crack along the upper beam/adhesive bond interface. Crack length is inferred from specimen compliance, and the specimen is unloaded and reloaded during the test to establish the crack length during the loading step.

2.1. Adhesively Bonded Asymmetric Double Cantilever Beam Specimen Designed to Measure the Toughness of an Al_2O_3/Epoxy Interface

Previous work aimed at measuring the toughness of aluminum/epoxy interfaces [4] provided a starting point for designing an ADCB specimen to measure the toughness of Al_2O_3/epoxy interfaces. There are four primary parameters to select when designing an adhesively bonded ADCB: beam Young's modulus E_1, E_2, and beam thickness h_1, and h_2 (see Figure 2). However, since the upper beam and

adhesive layer define the interface of interest, the only real material option available is the choice of the lower beam material. For this study it was decided to use Kovar as the lower material since its coefficient of thermal expansion (CTE) is a good match to that of a 94 percent Al_2O_3 (material data sheets indicate that both have a CTE of ~ 5 μm/m per °Celsius (C) over a temperature range of 25 °C to 200 °C). This choice avoids a CTE mismatch that could introduce residual bending stress in the ADCB as the epoxy is cooled from its elevated cure temperature to the test temperature. Residual bending stress can generate crack opening (or closing) that is difficult to account for and this can introduce uncertainty in the data reduction.

Once the lower and upper beam materials are selected, the only design choice remaining is the lower beam's thicknesses. Here Sandia National Laboratories desires an ADCB specimen design that produces a predominantly Mode I-like loading near the crack-tip since SNL is interested in measuring a value that is close to the lower bound of the interfacial toughness (see Figure 1). The challenge is to choose a beam thickness that generates cracking along the Al_2O_3/epoxy interface at a low crack-tip mode-mixity, while avoiding premature failure of the brittle Al_2O_3 beam, cohesive failure within the epoxy, or failure at the epoxy/Kovar interface. This can be particularly problematic if the epoxy or Kovar/epoxy interface toughness is less than that of the Al_2O_3/epoxy interface. There are competing effects that are often in conflict. For example, increasing the crack-tip mode-mixity for a crack on the Al_2O_3/epoxy interface by increasing the thickness of the Kovar beam will tend to push the crack towards the Al_2O_3 beam and help keep the crack on the desired interface. However, as shown in Figure 1, increasing the mode-mixity also increases the interfacial toughness, making the other failure modes more likely.

To aid in the design effort, a solution developed by Suo and Hutchinson [10] for a semi-infinite interface between two infinite isotropic elastic layers under general edge loading conditions was specialized to the ADCB geometry and coded into a spreadsheet (see Appendix A Spreadsheet To Aid in the Design of ADCB Specimens). This solution determines the energy release rate G for an increment of crack growth along the interface as a function of applied load P, crack length a, beam width w, Young's modulus E_1, E_2, Poisson's ratio ν_1, ν_2, and beam thickness h_1, h_2 (see Figure 2). Furthermore, additional results by Suo and Hutchinson [11] were used to estimate the crack-tip mode-mixity. This analysis determined a universal relation for mode-mixity that applies to a crack along the interface of a thin elastic layer that has been inserted into a homogeneous body. Although this solution

is not rigorously applicable to the adhesively bonded ADCB considered here (since the two beams are of different materials), it is noted that both materials are essentially rigid compared to the epoxy bond and consequently the analysis is expected to be applicable. As discussed in the Introduction section, the value of the crack-tip mode-mixity depends on the characteristic length used in its definition (i.e., $\psi_{r=l}$ is defined as the arctangent of the ratio of the shear stress to normal stress at a fixed distance l in front of the crack tip when l is within the region dominated by the crack-tip stress singularity). Fortunately, mode-mixity can be easily translated from one characteristic length scale to another [5]. The spreadsheet in Appendix A presents mode-mixity values defined at three characteristic length scales: h_1, bond thickness t, and a material length scale l_o. The material length scale l_o is perhaps the most illuminating since it defines mode-mixity at the scale where failure occurs (typically taken to roughly equal the length of the crack-tip yield zone, which for an epoxy is ~1- 10 μm). Note that you can only use the spreadsheet to compare various design options; there is insufficient failure data to make definitive predictions (note that the ADCB geometry that is being designed is to measure the unknown interfacial toughness).

Guided by the spreadsheet analysis and validated by testing, two ADCB specimen designs suitable for measuring the toughness of an Al_2O_3/epoxy interface have been identified. Both designs have a 0.1 inch (2.5 mm) thick, 94 percent Al_2O_3 upper beam, while the lower Kovar beam is either 0.138 inch (3.5 mm) or 0.185 inch (4.7 mm) thick. Both designs have a 0.02 inch (0.5 mm) thick adhesive bond layer. The bending stiffness of the upper and lower beams in the 0.138-inch-thick Kovar design are nearly matched with the bending stiffness of the Kovar beam about 20 percent higher. This generates a low mode-mixity close to the crack-tip with $\psi_{r=10\,\mu m} = 1^o$. On the other hand, the bending stiffness of lower beam in the 0.185-inch-thick Kovar design is about a factor of three greater than that of the Al_2O_3 upper beam and this generates a slightly negative mode-mixity with $\psi_{r=10\,\mu m} = -10^o$. A negative mode-mixity will tend to push the crack towards the upper Al_2O_3/epoxy interface, and consequently this design might encourage cracking on the desired interface in cases where crack kinking off the interface is an issue. Furthermore, the residual epoxy adhesive layer that remains on the Kovar adherend after separation along the Al_2O_3/epoxy interface can induce bending in the Kovar beam, and such bending could have a modest impact on the accuracy of the data reduction methodology. The design with the thicker Kovar adherend would tend to mitigate this possibility. There is no claim that these two designs described in this SAND Report are optimal, but rather both designs have been used to successfully measure the toughness of an Al_2O_3/epoxy interface at their

respective crack-tip mode-mixity. Note that there is only moderate variation in measured toughness with crack-tip mode-mixity at low mode-mixity, so both designs should generate similar, but possibly somewhat different values of measured toughness (see Figure 1).

3. FABRICATION

Figure 3 shows an as-fabricated, adhesively bonded ADCB specimen with a 0.1-inch-thick Al_2O_3 upper beam and a 0.185-inch-thick Kovar lower beam. This section describes the process used to fabricate this specimen.

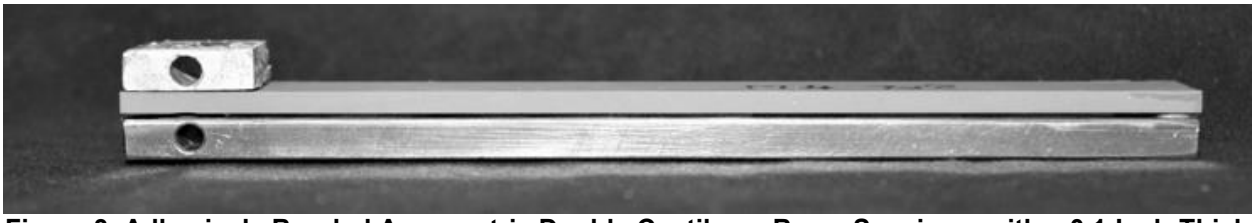

Figure 3. Adhesively Bonded Asymmetric Double Cantilever Beam Specimen with a 0.1-Inch-Thick Al_2O_3 Upper Beam and a 0.185-Inch-Thick Kovar Lower Beam.

Note: Also shown is a drilled block that is bonded to an upper beam prior to testing so that the upper beam can be pinned to the load train.

3.1. Adhesively Bonded Asymmetric Double Cantilever Beam Materials

1. Upper Al_20_3 Beam is shown in Figure 4.

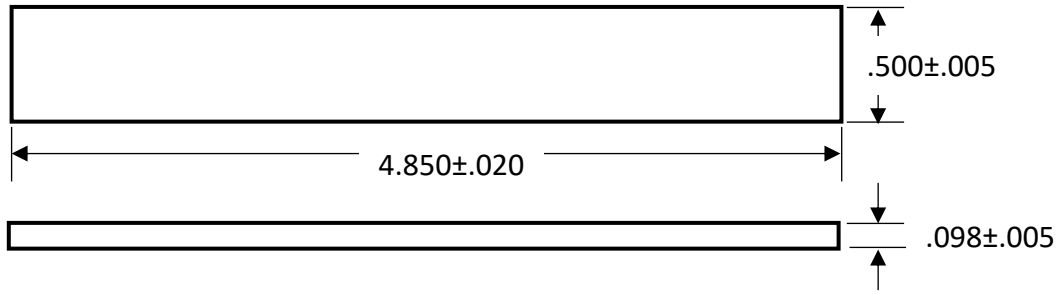

Figure 4. Drawing Defining Al_20_3 Upper Beam (Inches).

2. Lower Kovar beam, is shown in Figure 5. Do not break edges. No burrs allowed. Note that the two thru holes on upper surface are used to inject epoxy to for adhesive bond.

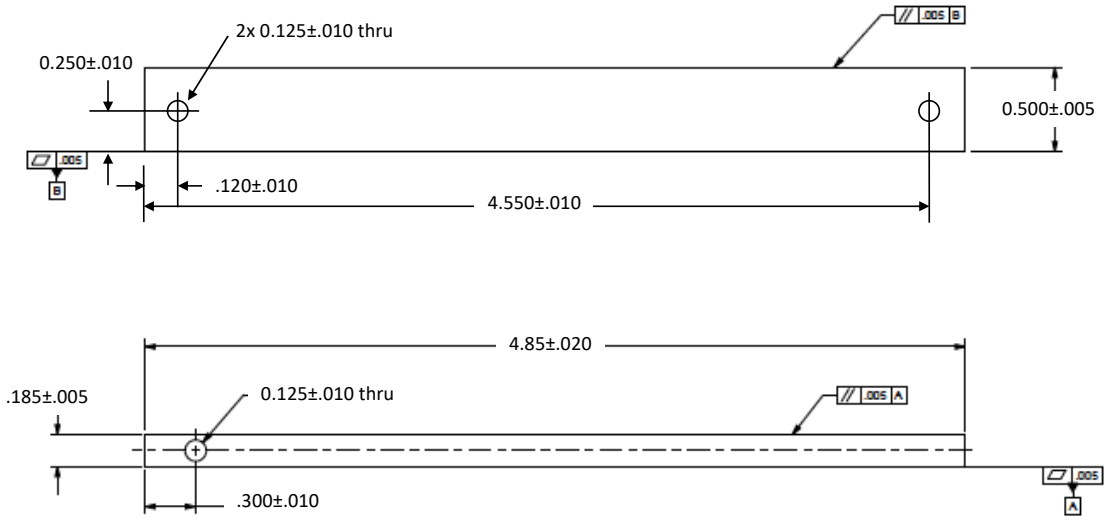

Figure 5. Drawing Defining Kovar Lower Beam (Inches).

3. Epoxy adhesive is: Diglycidyl ether of bisphenol A (EPON® Resin 828, Momentive) resin cured with diethanolamine (DEA, Sigma-Aldrich) at a 100:12 parts by weight mix ratio.

3.2. Process Al_2O_3 Beam

1. Roughen the Al_2O_3 Beam's Bonding SurfaceGrit blast the bonding surface with a Swam-Blaster, setting the pressure to 7 pounds per square inch (psi) and using AccuBrade-50, Blend #3 media. There are three different sweep patterns (~ -45°, 45° and circular; see Figure 6) and each sweep pattern is repeated three (3)times (i.e., three (3) sweeps/pattern).

2. Clean the Al_2O_3 beam's bonding surface. Blasting media is removed with a 10-minute sonication (Crest Ultrasonic Model 7-10-GPM setting 6). The beam is then treated with Brulin cleaner (BHC Inc), sonicated for 10 minutes, and rinsed with a stream of ultrahighpure (UHP) water (18.2mΩcm-1).

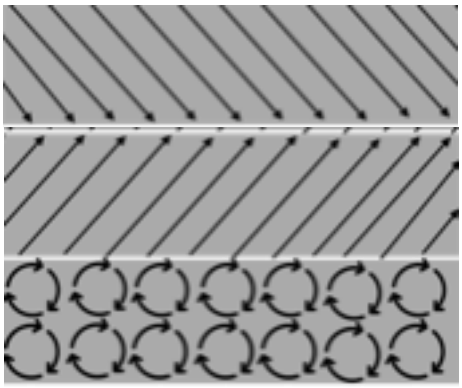

Figure 6. Pencil Blast Sweep Pattern: -45°, 45°, and Circular.

3. Silane coat the Al_20_3 beam.
   a. First apply a 1.5-inch length of Teflon tape to one end of the beam so that no silane is applied to this masked portion of the beam (this uncoated region is less tough, and this facilitates the insertion of the required initial crack).
   b. A 55° C preheated beam is coated with silane (3-aminopropyltrimethoxysilane, Aldrich) by chemical vapor deposition. The Al_2O_3 beam is placed on a shelf within a vacuum oven. A glass dish with approximately 1 mL of silane is also placed in the oven. Deposition occurs overnight at a vacuum of 10-15 in-Hg at 55°C (VWR model 1430M).

3.3. Process Kovar Beam

1. Roughen Kovar bonding surface. Uniformly roughen bonding surface by sandblasting with 60 grit garnet media (Vacublast International Model 270903) at 70 psi.

2. Clean Kovar beam's bonding surface. Blasting media is removed with a 10-minute sonication (Crest Ultrasonic Model 7-10-GPM setting 6). The beam is then treated with Brulin cleaner (BHC Inc), sonicated for 10 minutes, and rinsed with a stream of UPH water (18.2mΩcm-1).

3. Silane coat Kovar beam.
   a. A 55° C preheated beam is coated with silane (3-aminopropyltrimethoxysilane Aldrich) by chemical vapor deposition. The Kovar beam is placed on a shelf within a vacuum oven. A glass dish with approximately 1 mL of silane is also placed in the oven. Deposition occurs overnight at a vacuum of 10-15 in-Hg at 55°C (VWR model 1430M).
   b. The Al_2O_3 beams and the Kovar beams can be silane coated simultaneously (i.e., placed in the same oven and coated at the same time).

3.4. Adhesively Bond Beams to Form ADCB Specimen

1. Clean beams prior to bonding.
   a. Remove the Teflon mask from the Al_2O_3 beam and mark this end of beam (need to know which end of the Al_2O_3 beam is without the silane coating during bonding operation).
   b. Apply sequential rinses with reagent grade toluene, acetone, and UHP water ($18.2M\Omega cm^{-1}$).
   c. Dry beams between solvent rinses with a stream of UHP Nitrogen gas.

2. Apply 0.02-inch spacers (Artus 0.02 inch-0.5mm yellow) to the four corners of the Kovar beam's bonding surface.

3. Stack Al_20_3 and Kovar beams (separated by the spacers bonded to the Kovar) and then apply Teflon tape edges to form bond cavity.
   Note that roughened Al_2O_3 and Kovar bonding surfaces face each other across the bond cavity.
   Also note that the end of the Al_2O_3 beam that was not silane coated (the end marked in step 3.4.1.a) is bonded to the end of the Kovar beam that has the thru hole used to pin the ADCB to the load train.

4. Apply approximately one-inch (1") square dam of pink solder mask (Wonder Mask P Techspray part no 2211 CIS AQ10059402) around Kovar beam thru holes to create reservoirs for epoxy overflow.

5. Preheat beams to 71°C.

6. Mix epoxy.
   a. Hand mix the EPON® Resin 828 resin and DEA curing agent for two to three (2 to 3) minutes at a ratio of 100:12 parts by weight epoxy to curing agent then degassed at 1-3 torr for three (3) minutes at 71°C.
   b. The epoxy is poured into 10CC syringes fitted with SmoothFlow 60° beveled tips (Nordsom 14GATT PN 7018052; trimmed to fit fill hole).

7. Inject epoxy into fill hole until the epoxy is ejected from the second overfill hole (see Figure 5). The pink solder mask dams are used to contain the epoxy overfill at both ends and to allowed for cure shrinkage.

8. Cure using prescribed epoxy cure schedule.

4. TEST PROCEDURES

Figure 7 shows an ADCB specimen pinned to loading fixturing prior to testing. The lower clevis is hard mounted to the load frame's fixed base, while as steel chain is used to attach the upper clevis to the load cell and moving crosshead.

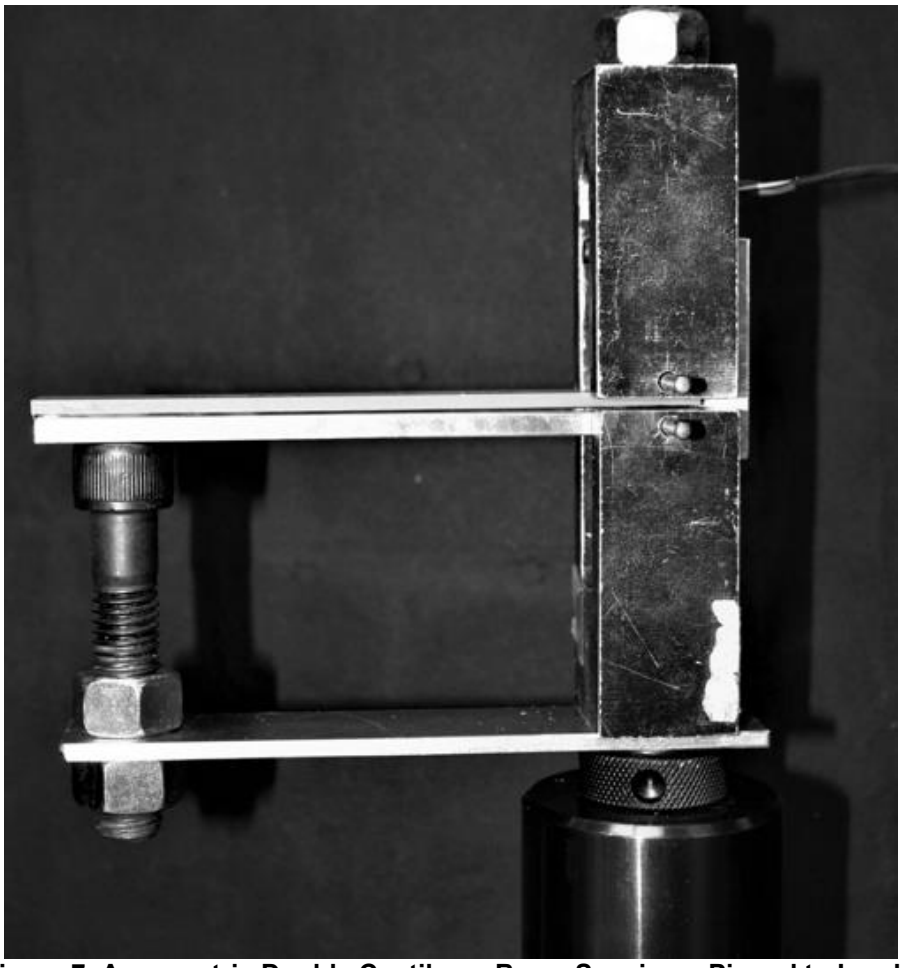

Figure 7. Asymmetric Double Cantilever Beam Specimen Pinned to Load Train.

4.1. Pre-crack Asymmetric Double Cantilever Beam and Bond on Clevis Adaptor Block

1. Saw past pin holes using wet saw ~ 0.02-inch-thick blade.
2. Use jeweler saw to cut chevron notch along Al_2O_3 surface.
3. Use thin razor blade with diamond paste to extend crack along Al_2O_3 surface.
4. Clamp sample in vise with about 1.25 inch of the crack end outside vise. Carefully pry open crack with thin blade screwdriver.
5. Clevis adaptor block (an aluminum block with nominal dimensions of 0.5-inch-wide by 0.6-inch-long by 0.2-inch-thick) is used to attach the ADCB specimen to the top clevis. It is bonded to Al_2O_3 beam using a cyanoacrylate adhesive. The Linear Variable Differential Transformer (LVDT) holder bracket is used to hold the LVDT that measures crack opening

displacement. It is also bonded to the bottom of the Kovar beam sample using the same cyanoacrylate adhesive (see Figure 8).

4.2. Test Set Up

1. Instron load frame with a 200-foot pound force (lbf) load cell.
2. Assemble fixturing used to attach ADCB to Instron (see Figure 7) and apply small preload (~0.5 lbf).
3. Instrumentation and calibration.
   a. Measure applied load using a 200 lbf load cell.
   b. Load-point displacement is continuously recorded using a LVDT (Schaevitz MHR050, calibrated to a +/- 0.100-inch range) with a conditioning unit (ATA-2001).
   c. LVDT is attached to the ADCB using the LVDT holder (see Figure 8).
   d. Adjust the LVDT output voltage reading to approximately 0V before tightening the set screw.

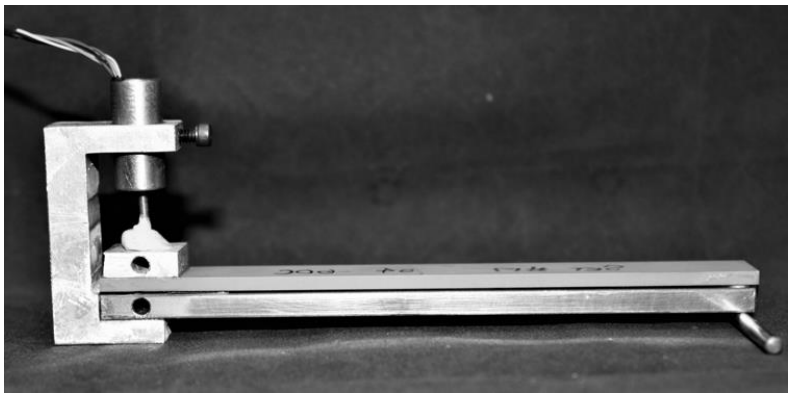

Figure 8. ADCB Sample Mounted in LVDT Holder.

4. Calibration: Confirm that load cell and LVDT is calibrated by using standard procedures.

4.3. Data Acquisition

1. Crosshead displacement rate is 0.05 inch/minute.
2. Load, crosshead displacement, and LVDT readings are taken with an external data acquisition (DAQ) system. The DAQ system consists of a voltage input unit and a LabVIEW program.
3. Apply multiple load/unload steps to propagate crack by a small increment during each step by programing in displacement steps.
4. The test is terminated when sample breaks or when at the maximum 0.1-inch displacement that can be measured.
5. The raw data collected by LabVIEW is copied into an Excel spreadsheet. The LVDT displacement data is adjusted so that the displacement at time zero is zero. The load data reflects the initial ~ 0.5 lbf preload.

5. DATA REDUCTION

5.1. Theory

The ADCB test does not measure interfacial toughness Γ directly. Instead, the load vs. load-point displacement data measured during the ADCB test is used to determine: 1) specimen stiffness prior to crack propagation and 2) the load at which the crack begins to propagate. This information is then used in conjunction with analytical results for the ADCB to determine the critical value of the energy release rate G_c when the crack begins to propagate (by definition, $\Gamma = G_c$). The energy release rate G for an ADCB specimen can be derived using beam theory, and for the case of an ADCB composed of two beams of differing materials and thickness.

Equation 1

$$\boldsymbol{G = (Pa)^2 F(a)/(2wEI)}$$

where:

P = applied load

a = crack length

w = beam width

h_1 = upper beam height

E_1 = upper beam Young's modulus

h_2 = lower beam height

E_2 = lower beam Young's modulus

$EI = (1/(EI)_1 + 1/(EI)_2)^{-1.}$

$(EI)_1 = wE_1h_1^3/12$

$(EI)_2 = wE_2h_2^3/12$

$F(a) = EI((1+0.64h_1/a)^2/(EI)_1 + (1+0.64h_2/a)^2/(EI)_2)$

Note that *F(a)* is a correction factor that accounts for the transverse stiffness of the beams. The correction factor for the ADCB specimen geometry used here is based on a straight-forward extension of published results for a one material DCB (those results were based on an analysis of a beam on an elastic foundation. [12]).

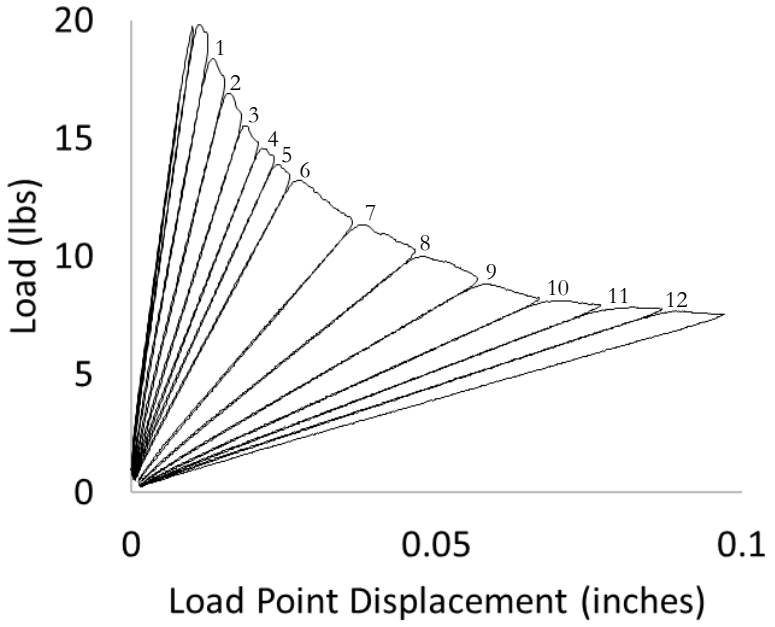

Figure 9. Example of the Measured Load vs. Load-Point Displacement Data.
Note: This example is for an adhesively bonded ADCB with a 0.1-inch-thick 94 percent Al_20_3 upper beam and a 0.185-inch-thick Kovar lower beam with a .02-inch-thick epoxy bond.

Since all of the ADCB's geometric and elastic properties are known, all that one needs to know to determine G_c is the current crack length a and the critical load P_c at which this crack propagates. Figure 9 shows an example of the measured load vs. load-point displacement relationship for an adhesively bonded, ADCB with a 0.1-inch-thick 94 percent Al_2O_3 upper beam and 0.185-inch-thick Kovar lower beam (0.02-inch-thick epoxy bond). To highlight a typical crack growth step, Figure 10 shows the loading portion of the curve corresponding to step 6 in Figure 9. During loading, the load vs. load-point displacement is essentially linear over much of its range, and clearly deviates from linearity when the crack begins to propagate.

The loading stiffness *K* is defined as the slope of the linear portion of the loading curve (see Figure 10, K has units of lb/in).

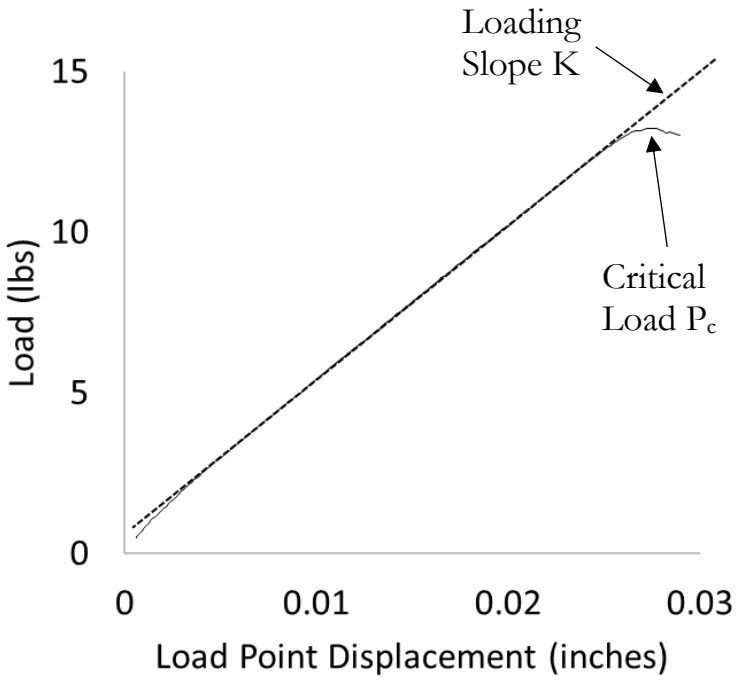

Figure 10. Definition of Loading Slope and Critical Load.
Note: See Load 6 in Figure 9.

As the crack grows, the length of the ADCB arms increase and the specimen stiffness decreases (i.e., for the same applied load, the load point displacement increases as the crack length increases). Consequently, one can use the same sort of beam theory analysis as used to determine *G* to determine crack length *a* using the measured loading stiffness *K* (substitute Eq. 1 in the integration of the fracture mechanics relationship $G = \frac{1}{2}P^2\frac{dC}{da}$, where specimen compliance C = 1/K). Crack length is related to *K* by:

Equation 2

$$a = \left(\frac{3EI}{K}\right)^{\frac{1}{3}} - 0.64EI\left(\frac{h_1}{(EI)_1} + \frac{h_2}{(EI)_2}\right)$$

where all equation parameters were defined above. The critical load P_c can be read directly from the measured load vs. load-point displacement data. In Figure 10 the curve bends over and reaches a peak load soon after it deviates from linearity. The value of P_c is set equal to this peak load P_{max}. As an

illustration, Table 1 lists P_c and K values for the data plotted in Figure 9. Example of the Measured Load vs. Load-Point Displacement Data. Note that the deviation from linearity prior to peak load can be caused by crack-tip plasticity, subcritical crack growth, etc. [1]. For brittle interfaces, the deviation prior to peak load should be limited and is considered a relatively small effect. For example, in Figure 10 a secant line that passes through P_c has a slope equal to ~0.95K and this reduced slope corresponds to less than a 2 percent increase in crack length. This potential increase in a during subcritical crack growth introduces only a small amount of uncertainty in the calculated G_c (less than a 4 percent). Note, however, if there were a significant increase in load during subcritical cracking than the validity of the calculated G_c is in question (e.g., if the load at the intersection of a 0.95K secant line and P_{max} differ by more than 10 percent).

Table 1. Critical Load and Loading Slope Data.
Note: This is data plotted from Figure 9.

Loading	Critical Load (lb)	Slope (lb/in)
1	18.39	1375
2	16.90	1046
3	15.52	812
4	14.57	662
5	13.87	573
6	13.21	484
7	11.30	299
8	9.98	211
9	8.81	152
10	8.09	118
11	7.77	99
12	7.66	86

5.2. Procedure

1. Measure upper and lower beam thicknesses, beam width, and bond thickness.
2. Elastic properties of beams are assumed to be known (provided that reliable handbook values are available).
3. Determine loading slope and critical load for each load/unload step. A typical ADCB test will have ten or more load/unloading steps (see Figure 9). Skip the first loading step since the

initial inserted crack may not be sharp and a sharp crack is required for a valid G_c measurement (propagated cracks should be sharp).

4. Paste P_c and K values into spreadsheet shown in Appendix B: Spreadsheet that Calculates Toughness (spreadsheet calculations based on results presented in Section 5.1)
5. Spreadsheet displays calculated toughness values Γ ($\Gamma = G_c$) for each loading step as well as average of all calculated toughness values, the standard deviation, and 95 percent confidence interval on the mean value.

Note that the measurement is valid only when:

1. The crack propagates along the upper beam/epoxy interface (i.e., along the Al_2O_3/epoxy interface).
2. The measured load vs. load-point displacement data has the same general appearance as that shown in Figure 9. Specifically, the unloading curve of one cycle and the loading curve of the next should have similar slopes and only a small offset. Figure 11 shows an example of questionable load vs. load-point displacement data.

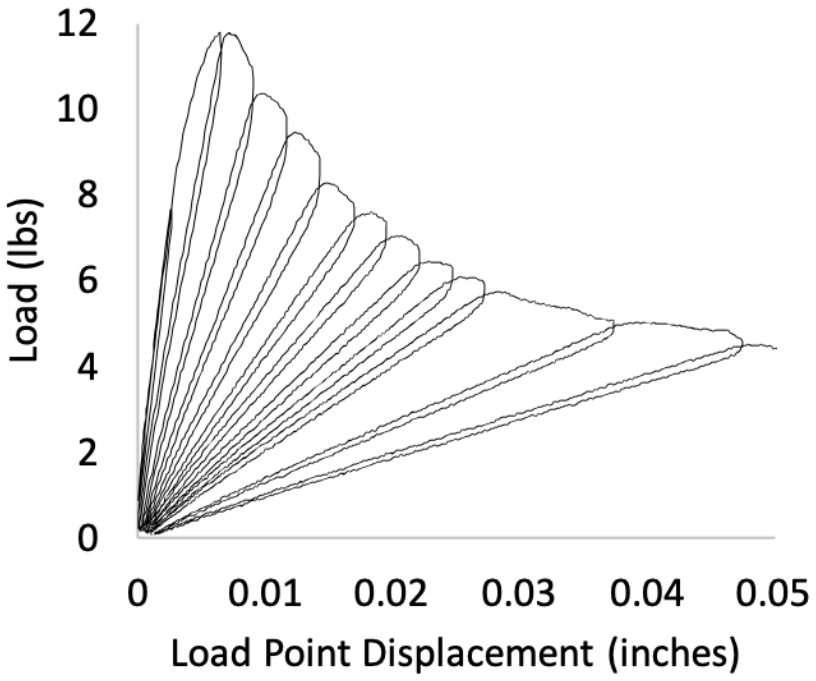

Figure 11. Example of a Questionable Load vs. Load-Point Displacement Data.
Note: This figure shows undesired frictional unloading/loading loops.

The unloading/loading loops are significant in Figure 11, and this is thought to be a result of friction between the clevis and the pinned ADCB (friction can cause some of the applied load

to bypass the specimen). If such loops are observed, discontinue the test and re-pin specimen to the clevis in a way that reduces specimen/clevis interference.

6. EXAMPLE ASYMMETRIC DOUBLE CANTILEVER BEAM-MEASURED AL_2O_3/EPOXY TOUGHNESS DATA

The motivation for developing an ADCB-based approach for measuring the toughness of an Al_2O_3/epoxy interface is a desire to develop a capability that can quantify how various processing choices effect interfacial bonding. To illustrate this capability, results for interfaces with or without a silane coating on the Al_2O_3 surface are presented here. The ADCB specimens used in these tests had a 0.1-inch-thick, 94 percent Al_2O_3 upper beam and 0.185-inch-thick Kovar lower beam. The nominal epoxy bond thickness was 0.02 inch thick. Figure 12 plots the measured interfacial toughness of an Al_2O_3/epoxy interface.

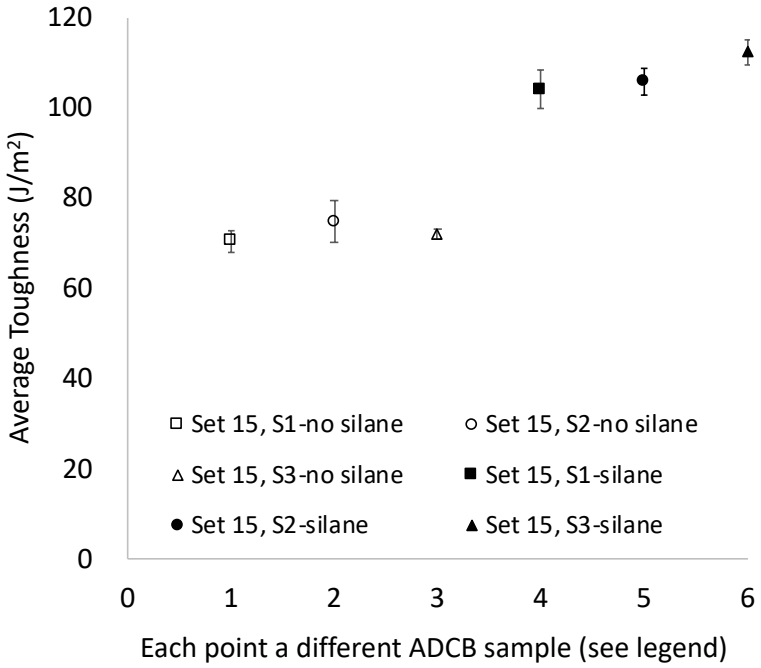

Figure 12. Measured Interfacial Toughness of an Al_20_3 Epoxy Interface: Average.

Note: The Al_20_3 is either coated or not coated with silane. Each symbol is the average of all Γ values measured in a single ADCB test and the error bars are +/- one standard deviation.

A total of six ADCB specimens were fabricated and tested in accordance to the procedures describe in Sections 3 Fabrication and Section 4 Test Procedures with the exception that no silane coating was applied to three (3) of the six (6) specimens tested. Figure 12 summarized the measured toughness data. Each symbol is the average of all Γ values measured in a single ADCB test and the error bars are +/- one standard deviation. The interface with the silane coated Al_2O_3 has a consistently higher toughness, with a Γ of ~ 110 J/m^2, while the interface with the uncoated Al_2O_3 has a Γ of ~ 70 J/m^2. The error-bars in the plot correspond to +/- one standard deviation.

The variability in the measured Γ values is illustrated in Figure 13.

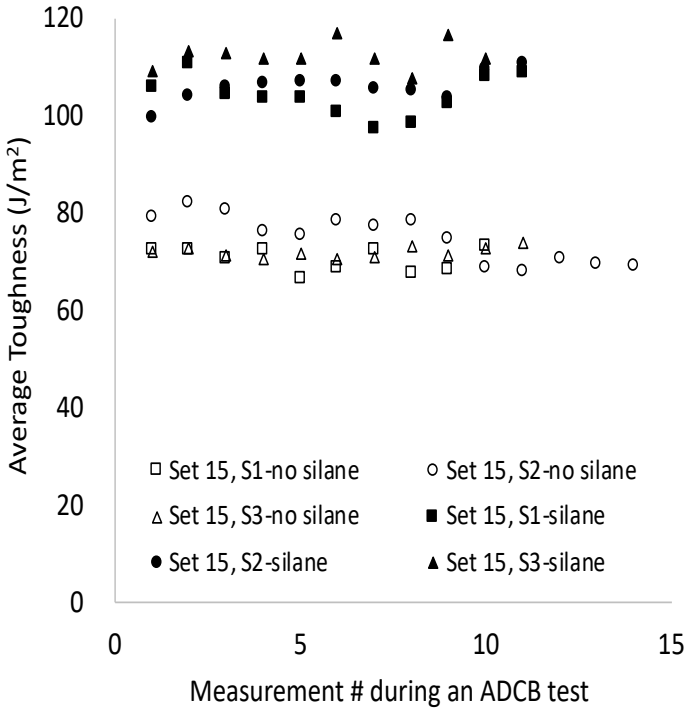

Figure 13. Measured Interfacial Toughness of an Al_20_3/Epoxy Interface: All Data Points.

Note: The Al_20_3 is either coated or not coated with silane. All Γ values measured during an ADCB test are plotted (each symbol corresponds to a different ADCB test).

Here all the Γ values measured during an ADCB test are plotted for each specimen tested (each symbol corresponds to a different ADCB test, where each measurement number corresponds to a different loading cycle, see Figure 9). This shows that there is no observable bias in the data measured at different crack lengths.

This page left blank

7. CONCLUSION

Although this SAND Report is focused on describing an ADCB-based methodology to measure the interfacial toughness of an Al_2O_3/epoxy interface, it may be possible to modify and adapt this methodology so as to measure the toughness of an interface between other materials. However, it should be emphasized that the techniques described here presume the applicability of LEFM concepts [1, 2]. In particular, it is assumed that there is only small-scale crack-tip yielding. One useful estimate for the crack-tip plastic zone size R_p can be made for the case where one material is much stiffer than the other (e.g., interface between a metal or ceramic and an epoxy). In such cases, the stiffer material can be assumed to be rigid and a plane strain estimate for R_p can be made in a way that is analogous to that used for a crack in a homogeneous material [13]. Specifically

Equation 3

$$R_p = \frac{1}{3\pi}\left[\frac{2\bar{E}\Gamma}{(1-\beta^2)\sigma_y^2}\right] \qquad \text{where} \qquad \beta = \frac{(1-2\nu)}{2(1-\nu)} \quad \text{and} \quad \bar{E} = \frac{E}{(1-\nu^2)}$$

where for the compliant material E is Young's modulus, ν is Poisson's ratio, and σ_y is the yield strength. For example, the results reported in Section 6 Example Asymmetric Double Cantilever Beam-Measured Al_2O_3/Epoxy Toughness Data are for an EPON® Resin 828/DEA epoxy with an E=3 GPa, ν = 0.38, and σ_y = 100 MPa. If the interface toughness Γ = 100 J/m^2 (i.e., a Γ value similar to that reported in Section 6, Figure 12), then R_p = 7.7 micrometers. This value of R_p is much small than the 0.5 mm thick adhesive bond used in the ADCB specimen and thus LEFM should apply. One should proceed with care and assess the applicability of LEFM before adapting the procedures presented in the SAND Report to new classes of material pairs. Also note that since Γ is unknown prior to testing, specimen design may be an iterative process.

This page left blank

APPENDIX A. SPREADSHEET TO AID IN THE DESIGN OF ADCB SPECIMENS

This spreadsheet calculates energy release rate, mode-mixity, and maximum upper beam stress for prescribed ADCB applied load, crack length, beam elastic properties, and beam thicknesses.

	A	B	C
	Based onSuo, Z.G. and J.W. Hutchinson, INTERFACE CRACK BETWEEN 2 ELASTIC LAYERS. International Journal of Fracture, 1990. 43(1): p. 1-18.		
	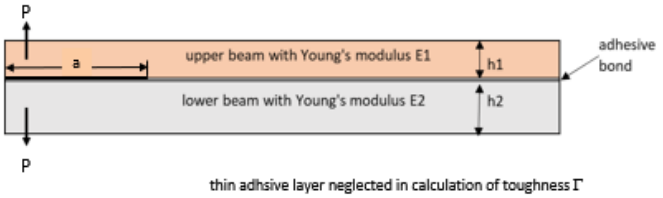		
	thin adhsive layer neglected in calculation of toughness Γ		
1			
2	**Input quantities Bold**	define cell values listed in column A	set14 sample1
3	**P - load when crack begins to propagate (N)**		**65.2**
4	**a - crack length (mm)**		**38.8**
5	**w - beam width (mm)**		**12.7**
6	**E1 - upper beam Young's modulus (MPa)**		**318000**
7	**nu1 - upper beam Poisson's ratio**		**0.21**
8	**h1 - upper beam height (mm)**		**2.5**
9	**E2 - lower beam Young's modulus (MPa)**		**138000**
10	**nu1 -lower beam Poisson's ratio**		**0.32**
11	**h2 - lower beam height (mm)**		**3.5**
12	**t = bond thickness (mm)**		**0.5**
13	**lo - material characteristic length (mm)**		**0.01**
14			
15	G1 (MPa, shear modulus)	=E1/(2*(1+nu1))	131405
16	kap1 (plane stress)	=(3-nu1)/(1+nu1)	2.31
17	c1	=(1+kap1)/G1	2.52E-05
18	G2 (MPa, shear modulus)	=E2/(2*(1+nu2))	52273
19	kap2 (plane stress)	=(3-nu2)/(1+nu2)	2.03
20	c2	=(1+kap2)/G2	5.80E-05
21	Gamma	=G1/G2	2.5138
22	alpha	=(Gamma*(kap2+1)-(kap1+1))/(Gamma*(kap2+1)+(kap1+1))	0.3947
23	beta	=(Gamma*(kap2-1)-(kap1-1))/(Gamma*(kap2+1)+(kap1+1))	0.1176
24	eps	=(1/(2*PI()))*LN((1-beta)/(1+beta))	-0.0376
25	Sigma	=(1+alpha)/(1-alpha)	2.3043
26	eta	=h1/h2	0.7143
27	A	=(1+Sigma*(4*eta+6*eta^2+3*eta^3))^-1	0.0583
28	I	=(12*(1+Sigma*eta^3))^-1	0.0453
29	gam (radians)	=ASIN(6*Sigma*eta^2*(1+eta)*SQRT(A*I))	0.6705
30	M/w ((N-mm)/mm, moment/width)	= P*a/w	193.2
31	**omega (degrees, for alumina/kovar ADCB; see note 1)**		**49**
32	**chi - (degrees, for rigid/epoxy; see note 2)**		**-13**
33	**eps_r (for rigid/epoxy, assume plane strain; see note 3)**		**-0.06**
34			
35	**Calculated Energy Release Rate**		
36	**G (energy release rate) N/mm**	=1000*(c1/16)*((M/w)^2/(I*h1^3))	**88.15**
37			
38	**Mode-mixity**		
39	**psi(r=h1) (deg, plane stress, no adhesive bond)**	=ATAN(-COS(gam+omega/180*PI())/SIN(gam+omega/180*PI()))	**-2.6**
40	**psi(r=t) (deg, plane stress, no adhesive bond; see Note 3)**	=(psi(r=h1)*PI()/180+eps*LN(t/h1))*180/PI()	**0.9**
41	**psi_bond(r=t) (deg, plane stress includes adhesive bond, see Note 2)**	=psi(r-t)+chi	**-12.1**
42	**psi(r=lo) (deg, plane strain includes adhesive bond, see Note 3)**	=(psi_bond(r=t)*PI()/180+eps_r*LN(lo/t))*180/PI()	**1.3**
43			
44	**Maximum tensile bending stress in the upper beam**		
45	**s_max (Mpa)**	=6*(P*a/) / (w*h1^2)	**191.2**
46			
47	Note 1. The mode mixity value psi(r=h1, plane stress) listed in row 39 does not include the presence of the thin epoxy bond. Suo, Z.G. and J.W. Hutchinson (in INTERFACE CRACK BETWEEN 2 ELASTIC LAYERS. International Journal of Fracture, 1990. 43(1): p. 1-18) present Tables that lists the value of the parameter omega used in determining psi when the bond is neglected. Omega depends on elastic properties (alpha, beta in rows 22, 23) and relative beam thickness (eta in row 26). Omega =49 for an alumina/kovar ADCB(alpha=0.4, beta=0.1, eta=0.7). One can use these Tables to estimate Omega for other ADCB designs.		
48			
49	Note 2. Mode mixity value listed in rows 41 includes the presence of the thin epoxy bond. Suo, Z. and J.W. Hutchinson, (in Sandwich Test Specimens for Measuring Interface Crack Toughness. Materials Science and Engineering, 1989. A107: p. 135-143) have shown that one can account for the shift in mode mixity generated by a thin bond by including a shift in mode mixity. This shift depends on elastic properties (alpha, beta in rows 22, 23). The estimated shift factor generated whn the beams are much stiffer than the bond is -13 degrees.		
50			
51	Note 3. Mode mixity can be translated from one characteristic length scale to another using psi_2 = psi_1 + eps*ln(h2/h1). Eps value corresponds to that of the elastic materials on either side of the crack (value depends on if the bond is included, or not inluded).		
52			
53	note: some issues wrt to using sandwich correction to bimaterial since sandwich correction was derived for a homogeneous specimen. However, since both materials in the ADCB are essentailly rigid compared to epoxy, expect this shift is reasonable.		
54			
55	note: also some issues when go from plane stress at the specimen length scale to plane strain at the material length scale.		

This page left blank

APPENDIX B. SPREADSHEET THAT CALCULATES TOUGHNESS

This spreadsheet calculates toughness from measured load, loading-slope pairs for the prescribed ADCB beam materials and thicknesses.

	A	B	C	D	E	F	G	H	I	J	K	L
1	ADCB SPEC. DATA REDUCTION: adhesively bonded bimaterial beam											
2	use Reedy extended Kanninen correction for transverse beam compliance											
3	in calculation of crack length and toughness											
4		P, a, upper beam with Young's modulus E1, h1, adhesive bond, lower beam with Young's modulus E2, h2, P, thin adhsive layer neglected in calculation of toughness Γ										
5												
6	**Input quantities in bold**			can copy and past addional columns if more than 10 Crack data points (or remove columns if less)								
7	**Bold blue quantities: primary outputs**											
8			**Crack 1**	**Crack 2**	**Crack 3**	**Crack 4**	**Crack 5**	**Crack 6**	**Crack 7**	**Crack 8**	**Crack 9**	**Crack 10**
9	**P - load when crack begins to propagate (lbs)**		**30.10**	**30.10**	**30.10**	**30.10**	**30.10**	**30.10**	**30.10**	**30.10**	**30.10**	**30.10**
10	**K - measured loading stiffness (lb/in)**		**2365**	**2365**	**2365**	**2365**	**2365**	**2365**	**2365**	**2365**	**2365**	**2365**
11	**w - beam width (mm)**		**12.7**	**12.7**	**12.7**	**12.7**	**12.7**	**12.7**	**12.7**	**12.7**	**12.7**	**12.7**
12	**h1 - upper beam height (mm)**		**5**	**5**	**5**	**5**	**5**	**5**	**5**	**5**	**5**	**5**
13	**E1 - upper beam Young's modulus (MPa)**		**318000**	**318000**	**318000**	**318000**	**318000**	**318000**	**318000**	**318000**	**318000**	**318000**
14	**h2 - lower beam height (mm)**	define cell values listed in column A	**9**	**9**	**9**	**9**	**9**	**9**	**9**	**9**	**9**	**9**
15	**E2 - lower beam Young's modulus (MPa)**		**138000**	**138000**	**138000**	**138000**	**138000**	**138000**	**138000**	**138000**	**138000**	**138000**
16	EI_1	=w*E1*h1^3/12	4.21E+07	4.21E+07	4.21E+07	4.21E+07	4.21E+07	4.21E+07	4.21E+07	4.21E+07	4.21E+07	4.21E+07
17	EI_2	=w*E2*h2^3/12	1.06E+08	1.06E+08	1.06E+08	1.06E+08	1.06E+08	1.06E+08	1.06E+08	1.06E+08	1.06E+08	1.06E+08
18	EI (N-mm^2)	=(1/EI_1+1/EI_2)^-1	3.02E+07	3.02E+07	3.02E+07	3.02E+07	3.02E+07	3.02E+07	3.02E+07	3.02E+07	3.02E+07	3.02E+07
19	EI_lower/EI_upper	=EI_1/EI_2	2.5	2.5	2.5	2.5	2.5	2.5	2.5	2.5	2.5	2.5
20	P (N)	=4.45*P	133.9	133.9	133.9	133.9	133.9	133.9	133.9	133.9	133.9	133.9
21	C - compliance (mm/N)	=1/K*(25.4/4.45)	2.41E-03	2.41E-03	2.41E-03	2.41E-03	2.41E-03	2.41E-03	2.41E-03	2.41E-03	2.41E-03	2.41E-03
22												
23	**a - crack length (mm)**	=(3*EI*C)^(1/3)-0.64*EI*(h1/EI_1+h2/EI_2)	**56.3**	**56.3**	**56.3**	**56.3**	**56.3**	**56.3**	**56.3**	**56.3**	**56.3**	**56.3**
24	*CHECK: theory assumes a/h1>10*		11.26	11.26	11.26	11.26	11.26	11.26	11.26	11.26	11.26	11.26
25	To – toughness (J/m^2; beam theory with no transverse compliance correction)	=1000*(P*a)^2/(2*w*EI)	74.22	74.22	74.22	74.22	74.22	74.22	74.22	74.22	74.22	74.22
26	**Γ - toughness (J/m^2; includes correction for transverse beam compliance)**	=To*EI*((1+0.64*h1/a)^2/EI_1 + (1+0.64*h2/a)^2/EI_2)	**84.96**	**84.96**	**84.96**	**84.96**	**84.96**	**84.96**	**84.96**	**84.96**	**84.96**	**84.96**
27				all data								
28			**Γ avg =**	**84.96**	(change range of average/st dev/CI so agrees with the number of data points)							
29	References		**std dev =**	**0.00**								
30	Tada, H., P.C. Paris, and G.R. Irwin, The stress analysis of cracks handbook. 1973.	95% confidence interval (CI) +/-		**0.00**								
31	Hellertown, PA: Delaware Research Corporation. (later editions available)			**upper CI**	**84.96**							
32	Lists Stress Intensity Factor for bimaterial beam (section 29.3)			**lower CI**	**84.96**							
33												
34	Kanninen, M.F., AUGMENTED DOUBLE CANTILEVER BEAM MODEL FOR STUDYING											
35	CRACK-PROPAGATION AND ARREST. International Journal of Fracture, 1973. 9(1): p. 83-92.											
36	Describes method to correct the homogeneous DCB calibration for transverse beam compliance.											
37	Reedy's extension for a bimaterial beam is based on these results. It turned out that											
38	for the AL2O3 ADCB, Reedy's and Kanninen's correction are nearly the same.											

This page left blank

This page left blank

REFERENCES

[1] Kanninen, M.F. and C.H. Popelar, *Advanced Fracture Mechanics*. 1985, New York: Oxford University Press.

[2] Anderson, T.L., *Fracture Mechanics: Fundamentals and Applications*. 3rd Edition ed. 2005: CRC Press.

[3] Pocius, A.V., *Adhesion and Adhesives Technology*. 1997, Cincinnati: Hanser Gardner Publications, Inc.

[4] Reedy, E.D., Jr. and M.E. Stavig, *Interfacial Toughness: Dependence on Surface Roughness and Test Temperature*. Submitted for publication, 2019.

[5] Hutchinson, J.W. and Z. Suo, *Mixed Mode Cracking in Layered Materials*, in *Advances in Applied Mechanics*, J.W. Hutchinson and T.Y. Wu, Editors. 1992, Academic Press. p. 63-191.

[6] Volinsky, A.A., N.R. Moody, and W.W. Gerberich, *Interfacial toughness measurements for thin films on substrates.* Acta Materialia, 2002. **50**(3): p. 441-466.

[7] Thouless, M.D., et al., *The Edge Cracking and Spalling of Brittle Plates.* Acta Metallurgica, 1987. **35**: p. 1333-1341.

[8] Swadener, J.G. and K.M. Liechti, *Asymmetric Shielding Mechanisms in the Mixed-Mode Fracture of a Glass/Epoxy Interface.* Journal of Applied Mechanics, 1998. **65**: p. 25-29.

[9] Brown, H.R., *Mixed-Mode Effects on the Toughness of Polymer Interfaces.* Journal of Materials Science, 1990. **25**(6): p. 2791-2794.

[10] Suo, Z.G. and J.W. Hutchinson, *Interface Crack between Two Elastic Layers.* International Journal of Fracture, 1990. **43**(1): p. 1-18.

[11] Suo, Z. and J.W. Hutchinson, *Sandwich Test Specimens for Measuring Interface Crack Toughness.* Materials Science and Engineering, 1989. **A107**: p. 135-143.

[12] Kanninen, M.F., *Augmented Double Cantilever Beam Model for Studying Crack-Propagation and Arrest.* International Journal of Fracture, 1973. **9**(1): p. 83-92.

[13] Tvergaard, V. and J.W. Hutchinson, *The influence of plasticity on mixed mode interface toughness.* Journal of the Mechanics and Physics of Solids, 1993. **41**: p. 1119-1135.

DISTRIBUTION

Email—Internal

Name	Org.	Sandia Email Address
S. E. Klenke	1550	seklenk@sandia.gov
A. Brundage	1554	albrund@sandia.gov
J. E. Bishop	1556	jebisho@sandia.gov
E. Corona	1558	ecorona@sandia.gov
J. M. Emery	1558	jmemery@sandia.gov
H. E. Fang	1558	hefang@sandia.gov
S. J. Grutzik	1558	sjgrutz@sandia.gov
K. N. Long	1558	knlong@sandia.gov
E. D. Reedy	1558	edreedy@sandia.gov
J. G. Cordaro	1833	jgcorda@sandia.gov
R. Jaramillo	1833	rkjaram@sandia.gov
J. Carroll	1851	jcarrol@sandia.gov
K. Strong	1851	ktstron@sandia.gov
J. R. McElhanon	1853	jrmcelh@sandia.gov
J. M. Kropka	1853	jmkropk@sandia.gov
M. E. Stavig	1853	mestavi@sandia.gov
M. A. El	2566	mael@sandia.gov
J. A. Quinn	2566	jefquin@sandia.gov
S. House	2576	shouse@sandia.gov
R. Tandon	2576	rtandon@sandia.gov
C. F. Brooks	2585	cfbrook@sandia.gov
J. W. Dugger	2585	jwdugge@sandia.gov
E. C. Larkin	2585	elarkin@sandia.gov
J. W. Foulk	8363	jwfoulk@sandia.gov
J. Ostien	8363	jtostie@sandia.gov
B. T. Werner	8363	btwerne@sandia.gov
Technical Library	01977	sanddocs@sandia.gov

This page left blank

Sandia National Laboratories

Sandia National Laboratories is a multimission laboratory managed and operated by National Technology & Engineering Solutions of Sandia LLC, a wholly owned subsidiary of Honeywell International Inc. for the U.S. Department of Energy's National Nuclear Security Administration under contract DE-NA0003525.